

Classification model for infectious lung diseases using convolutional neural networks on web and mobile applications

Kennedy Okokpujie^{1,2}, Alvin K. Agamah¹, Abidemi Orimogunje³, Ijeh Princess Adaora⁴,
Olusanya Olamide Omolara⁵, Samuel Adebayo Daramola¹, Morayo Emitha Awomoyi⁶

¹Department of Electrical and Information Engineering, College of Engineering, Covenant University, Ota, Nigeria

²Africa Centre of Excellence for Innovative and Transformative STEM Education, Lagos State University, Ojo, Nigeria

³Department of Electrical and Electronic Engineering, Redeemer's University Ede, Ede, Nigeria

⁴Department of Computer and Information Science, College of Science and Technology, Covenant University, Ota, Nigeria

⁵Department of Computer Engineering, College of Engineering, Bells University of Technology, Ota, Nigeria

⁶School of International Service, American University, Washington, USA

Article Info

Article history:

Received Jul 26, 2024

Revised Feb 24, 2025

Accepted Mar 26, 2025

Keywords:

Chest X-ray

Classification

Convolutional neural networks

Diagnosis

Lung disease

ABSTRACT

Accurate lung disease diagnosis in infected patients is critical for effective treatment. Tuberculosis, COVID-19, pneumonia, and lung opacity are infectious lung diseases with visually similar chest X-ray presentations. Human expertise can be susceptible to errors due to fatigue or emotional factors. This research proposes a real-time deep learning-based classification system for lung diseases. Three models of convolutional neural networks (CNNs) were deployed to classify lung illnesses from chest X-ray images: MobileNetV3, ResNet-50, and InceptionV3. To evaluate the effect of high interclass similarity, the models were evaluated in 3-class (Tuberculosis, COVID-19, normal), 4-class (lung opacity, tuberculosis, COVID-19, normal), and 5-class (tuberculosis, lung opacity, pneumonia, COVID-19, normal) modes. The best classification accuracy was attained by retraining MobileNetV3, which obtained 94% and 93.5% for 5-class and 4-class, respectively. InceptionV3 had the lowest accuracy (90%, 89%, 93% for 5-, 4-, and 3-class), while ResNet-50 performed best for the 3-class setting. These findings suggest MobileNetV3's potential for accurate lung disease diagnosis from chest X-rays despite the interclass similarity, supporting the adoption of computer-aided detection systems for lung disease classification.

This is an open access article under the [CC BY-SA](https://creativecommons.org/licenses/by-sa/4.0/) license.



Corresponding Author:

Kennedy Okokpujie

Department of Electrical and Information Engineering, College of Engineering, Covenant University

Ota, Nigeria

Email: kennedy.okokpujie@covenantuniversity.edu.ng

1. INTRODUCTION

Lung diseases are also known as pulmonary diseases, and the term is used to describe a condition or a group of conditions that affects the lungs and makes them more vulnerable to medical injuries [1]. It also affects the ability of the lungs to function properly. These conditions can affect various parts of the lungs, such as the bronchi, bronchioles, alveoli and lung tissue. Because of how complicated these diseases are and their similarities, symptoms alone cannot be used to diagnose them. Various methods, such as magnetic imaging resonance (MIR), computed emission tomography (CET), positron emission tomography, and chest X-rays, are used to analyze lung diseases [2]. However, Chest X-rays are more common because they are less expensive and readily available in most healthcare centers. Lung diseases have been a significant threat to the health of humans for as long as they have existed. These diseases affect individuals of all ages; hence, they

are a global concern. They are a significant cause of mortality and morbidity in the world, affecting majorly low-income and middle-income countries [3]. The severity of lung disorders varies, ranging from minor/self-limiting symptoms, such as influenza and the common cold, to life-threatening ones, such as bacterial pneumonia, lung cancer, lung opacity, asthma, and TB. [4]. These conditions disturb the tissues and airways of the lungs and make it more difficult for the lungs to function normally, resulting in serious health issues [5], [6]. In the context of global health, the sustainable development goals (SDGs) emphasized the importance of addressing health-related challenges. Some of the SDGs, such as health and well-being, are directly affected by lung diseases because they are a major cause of mortality and morbidity globally, and they contribute to the increasing burden of non-communicable diseases worldwide. However, lung diseases affect more than just an individual's health; they also impact healthcare systems, economic productivity, and society's well-being. The nations and global organizations must work together to prevent, diagnose, and treat lung diseases to meet SDG 3. By understanding the relationship between Respiratory health and sustainable development objectives, we can provide and implement systems and structures to develop a healthier future for everybody.

Recently, computer-aided diagnosis (CAD) systems have become handy in detecting and managing lung diseases [7], [8]. They have revolutionized the process of analyzing medical images such as chest X-rays. X-rays are very useful in medical imaging because they provide detailed insights into the anatomical structures of the lungs, making it easier to obtain a more precise identification of abnormalities such as nodules, opacity and other pathological changes. By using digital signal processing techniques for image filtering and noise reduction, in conjunction with digital image processing techniques, these images are then enhanced and analysed to provide better visuals of lung tissues. By integrating digital signals and digital image processing into CAD systems, radiologists and other medical practitioners can benefit from accurate and timely diagnosis. Also, they are help in identifying subtle abnormalities and this results in early diagnoses and improvement in patient outcomes.

Medical imaging technologies, such as X-rays and ultrasounds, have altered the process of medical diagnosis, allowing medical specialists to observe the inside structures of the human body non-invasively [9]. Furthermore, these photographs give vital insights into the interior architecture of the human body by physical inspection only [10]. It generates a vast volume of data for computer-aided diagnostic systems and deep learning algorithms. Integrating deep learning with medical imaging yields a sophisticated CAD system capable of analysing data, highlighting regions with anomalies or difficulties, and improving overall diagnosis accuracy. Significant progress has been recorded in the use of imaging technology in making diagnosis and other clinical decisions. Because they are widely available and non-invasive, chest X-rays are vital for assessing lung-related diseases, and among other technologies, X-rays are widely popular because they are readily available even in rural areas, thus making it easy to obtain scans [11]. These scans have been used to diagnose several lung-related diseases, such as COVID-19 [12], [13].

Deep convolutional neural networks (DCNN) are critical for automating and simplifying the diagnosis of lung illnesses. It is one of the tactics used in medicine to solve problems. A deep convolutional neural network is a type of deep learning model that can handle picture recognition tasks well due to its ability to learn. This model can also extract the hierarchal characteristics from raw picture data; hence, DCNNs have become a valuable tool in medical image analysis. The artificial neural network behaves similarly to a human in that it mimics the structure and function of the human cortex, allowing it to learn complicated patterns from collections of medical pictures. The initial layers of the DCNN detect fundamental elements such as edges and forms. Subsequent layers integrate these traits to recognise more complex patterns, resulting in object recognition. In medical imaging, DCNNs examine chest X-rays to discover patterns and anomalies and utilise this to diagnose diseases such as tuberculosis and lung opacity. Several DCNN models have been built and trained to recognize lung illnesses from chest X-rays. ChexNet, a well-known model developed by a team at Stanford University, was trained on a huge dataset to diagnose several lung diseases [14]–[16].

The ChexNet model employs a form of DCNN architecture called DenseNet. Several other examples of DCNN models have exhibited great accuracy, frequently surpassing standard diagnostic methods and giving a vital second opinion. Despite the excellent accuracy gained in the study, the challenge with DCNN remains that it takes multiple images and a long training time even with GPU support [17], [18]. Transfer learning is a machine learning technique for image classification that uses the information obtained from training a model on one job to enhance performance on another, but related task. It is advantageous when the target task has limited training data, since it allows the model to benefit from the rich feature representations learnt on a bigger dataset.

Transfer learning has emerged as a vital technique in medical imaging, enabling significant performance increases in tasks like as disease detection, organ segmentation, and medical image categorisation. Transfer learning, by using pre-trained models constructed on large-scale datasets from broad domains, such as natural photos or other medical datasets, greatly decreases the requirement for big, labelled

medical datasets, which are frequently costly and time-consuming. This approach significantly accelerates the training process, especially for tasks with limited data. Transfer learning often leads to better results on the new task than training from scratch, and it helps minimize computational costs, as training from scratch can be resource intensive.

In a recent study Loey *et al.* [19] proposed using a generative adversarial network (GAN) with deep transfer learning to detect COVID-19 in chest X-ray images, overcoming the lack of datasets by synthesising new images. The dataset contained 307 photographs from four classes. Three deep transfers models-AlexNet, GoogLeNet, and ResNet18-were investigated to minimise complexity and execution time. The study investigated three scenarios with varying class numbers. Testing accuracy was the key metric, with GoogLeNet achieving the highest accuracy of 80.6% (first scenario), 85.2% (second scenario), and 100% (third scenario).

This research Malik *et al.* [20] highlighted the growing importance of medical imaging, particularly chest X-rays, in healthcare. Researchers utilized chest X-ray datasets to develop AI models that can accurately detect COVID-19, pneumonia, and healthy cases. Advancements in technology have significantly improved the accuracy and efficiency of medical diagnoses, making these imaging techniques crucial for disease detection and clinical decision-making. In addition, Shibly *et al.* [21] obtained a classification accuracy of 97.36%, a sensitivity of 97.65%, and a precision of 99.28% in identifying persons impacted by COVID-19, highlighting the potential of these methodologies to help healthcare professionals validate their evaluations. The contribution of this study includes the following:

- Collected hybrid chest X-ray images for lung opacity, COVID-19, viral pneumonia, bacterial pneumonia, healthy individuals and tuberculosis.
- Improved chest radiography analysis by developing a model for lung illnesses using several sources of X-ray images.
- Integrated the created model into the Telegram conversation bot and web application.

2. METHOD

Timely and accurate identification of infectious lung disorders is crucial for providing effective patient care and managing these conditions. While chest X-rays offer an accessible and cost-effective approach for initial evaluation, conventional diagnostic techniques largely depend on the expertise of radiologists, which can be subjective and time-consuming. Figure 1 gives the framework of the CNN model developed from data acquisition to model evaluation.

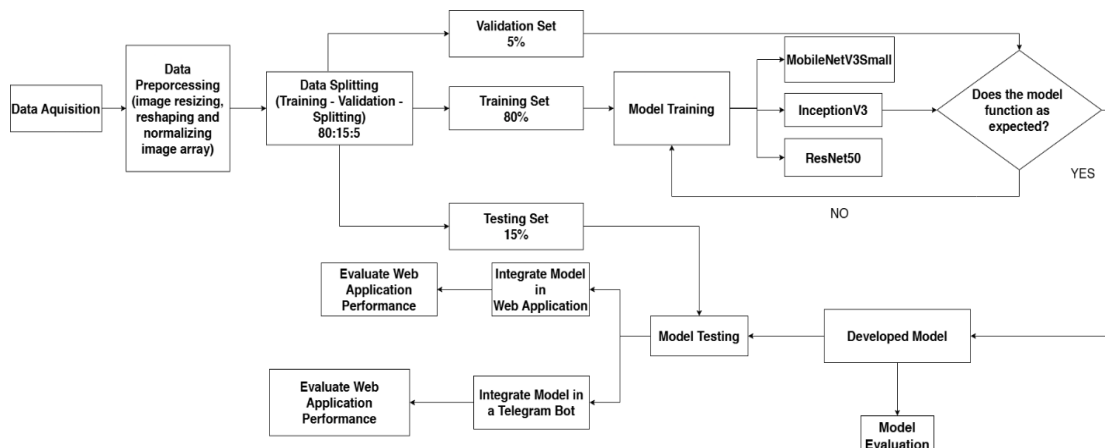


Figure 1. Conceptual framework of the developed model

In this work, sample images of lung diseases were taken from existing Kaggle repository [22], [23] and published journals [24]–[26] and the datasets are grouped into three. The first group of datasets was from a published work [21] which was also made available on Kaggle [23] and it has 3,616 X ray images of chests infected by COVID-19 containing 6,012 images of lung opacity and X ray images of 10,192 normal (non-infected) chests. The second group of datasets contain images of chests X ray infected by tuberculosis diseases with 3,500 chest images [22], [23]. The third group of datasets used in this work was obtained from

Kaggle repository and a published work. So, a total of 19,000 image datasets were employed, which were divided into five chest picture groups: COVID-19, lung opacity, TB, pneumonia, and normal chest. Each group has 3,800 data samples. As with a viable machine learning technique, the total datasets were divided into 75 % for the training, 20 % for the testing and 5% for the validation of the new model. The distribution of these datasets further shown in Table 1.

Table 1. Description of dataset

Classes	Total number of CXI	Training set	Validation set	Testing set
Tuberculosis	3800	3040	320	320
Pneumonia	3800	3040	320	320
Lung opacity	3800	3040	320	320
COVID-19	3800	3040	320	320
Normal	3800	3040	320	320

The batch normalisation algorithm from keras TensorFlow was used to normalise the input data before preprocessing the dataset. Each feature in the input array is normalised to a range of values between 0 and 1 after removing the mean value from the array and dividing the standard deviation of the features across the batch of data. To improve the performance and reliability of the model, the two parameters of batch normalization namely; the scale factor (γ) and shift factor (β) parameters were normalized during the data training.

Three cutting-edge pre-trained network architectures, MobileNetV3, ResNet50, and InceptionV3, were employed to extract deep features from the chest X-ray dataset. These network models were first pre-trained using the ImageNet dataset, which comprises one million pictures from 1000 classifications. In this study, the chest X-ray pictures were input separately into each of the pre-trained networks to extract feature vectors from the fully connected layers. All training and implementation took place in the Jupyter Notebook environment, using Python as the programming language. The MobileNetV3, ResNet50, and InceptionV3 models were developed using the TensorFlow 2.0 Keras framework, with training and experimentation done on the Google Collab platform.

In addition, the various datasets used in this work were preprocessed to a common size of 224 by 224 pixel for MobileNetV3 and ResNet50 models, 299 by 299 pixels for the Inception V3 Model. A transfer learning approach was employed with the MobileNetV3, ResNet50 and InceptionV3 models as base models, all of these were fine tuned to adopt the chest X ray datasets, and a view of this concept is shown in Figure 2. The feature extractions from the datasets and its fine tuning by the transfer learning methods helps in the performance improvement.

The model was trained for each model's five subclass classifications (tuberculosis, COVID-19, pneumonia, and lung opacity) and four subclass classifications (COVID-19, pneumonia, lung opacity, and TB). Each model has a batch size of 64, a dropout of 0.6, a learning rate of 0.001, global average pooling, and precise classification using the Adam optimiser. Figure 2 shows the transfer learning pathway.

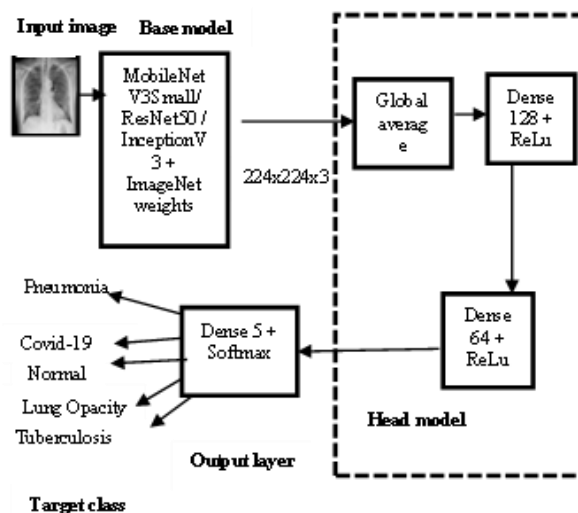


Figure 2. Transfer learning pipeline

The models were evaluated based on four criteria: accuracy, recall, precision, specificity, and the F1 score. They are described:

$$Accuracy = \frac{TP+TN}{TP+TN+FP+FN} \quad (1)$$

$$Precision = \frac{TP+TN}{TP+FP} \quad (2)$$

$$Recall = \frac{TP}{TP+FN} \quad (3)$$

$$F1\ Score = \frac{2*Precision*Recall}{Precision+Recall} \quad (4)$$

where: TP is true positive, TN is true negative, FN is false negative, and FP is false positive.

3. RESULTS AND DISCUSSION

3.1. Results

The higher the diagonal values in the confusion matrix, the more accurate the model's predictions were; conversely, the lower the off-diagonal values, the less frequently the model misclassified the data. The confusion matrix comprehensively evaluates the model's classification performance in all classes. This shows the strengths and weaknesses of the classification model while predicting lung disease.

3.1.1. 3-subclass classification models

This section explores the InceptionV3, ResNet-50 and MobileNetV3 performances for training and validation of losses, accuracies and as well as confusion matrix visualising on 3-subclass effectiveness in classifying pulmonary diseases from X-rays in a 3-subclass scenario (COVID-19, normal and tuberculosis) as depicted Figures 3-5. As shown in Figures 3(a), 4(a), and 5(a), InceptionV3 achieves an impressive overall accuracy of 93%, indicating it correctly classified 93% of the samples. Macro and weighted averages for precision, recall, and F1-score all reach 0.93, suggesting strong performance across all classes, even accounting for potential class imbalances. Firstly, the COVID class has the lowest score (88% precision, 95% recall, and 91% F1-score); indicating that the model may have some difficulty in accurately classifying COVID cases compared to the other classes. Then, the normal class achieved moderately high scores (93% precision, 89% recall, and 91% F1 score), indicating that the model can reasonably identify normal cases. Finally, the Tuberculosis class has the highest (99% precision, 95% recall, and 97% f1-score), suggesting that the model may have some challenges accurately classifying normal cases due to subtle variations within this category.

Figures 3(b), 4(b), and 5(b) show that on the 3-subclass classification task, ResNet50 performs impressively. With an overall accuracy of 91%, the model correctly identifies 91% of the samples in the dataset. The precision, recall, and F1-score macro and weighted averages all surpass 0.91, indicating strong performance in all classes. The weighted average also corrects for any potential imbalances in class. COVID-19: with scores of 92% precision, 97% recall, and 94% F1-score, the model performs exceptionally well in identifying COVID-19 instances. lung opacity: with 89% precision, 90% recall, and 90% F1-score, the model performs well in lung opacity situations. normal: with 92% precision, 87% recall, and 89% F1-score, the model performs the second worst on normal cases. This suggests some challenges in distinguishing subtle variations within this category.

MobileNetV3 results for 3-subclass classification are shown in Figures 3(c), 4(c), and 5(c). The overall accuracy of 90% indicates that the model correctly classified 90% of the samples in the dataset. Both macro and weighted average precision, recall, and F1-score are all 0.90, suggesting good average performance across all classes, with the weighted average additionally accounting for potential class imbalances. Firstly, the model performed well on COVID-19 classification with scores of 95% precision, 92% recall, and 93% F1-score. This suggests a good ability to identify COVID-19 cases. Secondly, the lung opacity class achieved moderately high scores (86% precision, 89% recall, and 88% F1 score), demonstrating the model's capability to identify lung opacity cases with reasonable accuracy. Finally, the model's performance in the normal class was the second lowest (89% precision, 88% recall, and 88% F1 score). This indicates some challenges in accurately classifying normal cases, potentially due to subtle variations within this category.

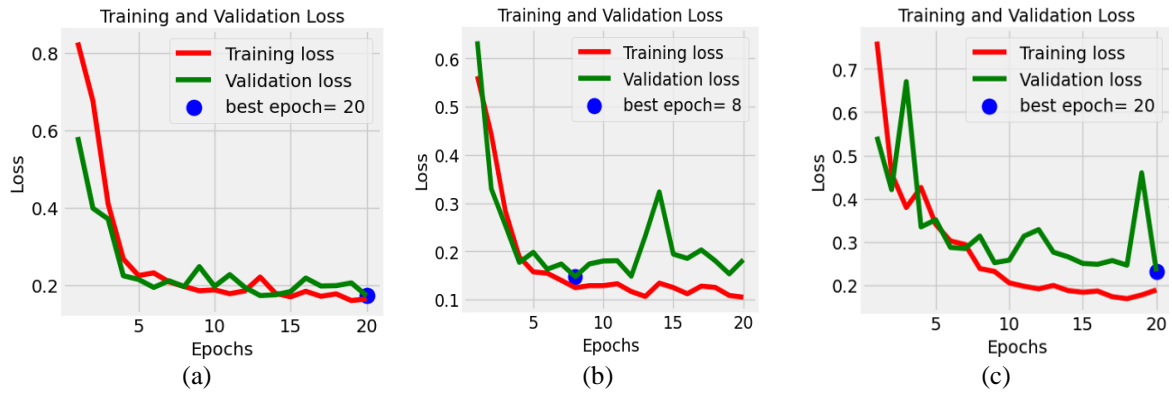


Figure 3. Chart visualizing: (a) InceptionV3, (b) ResNet-50, and (c) MobileNetV3 performances for training and validation losses on 3 Subclass

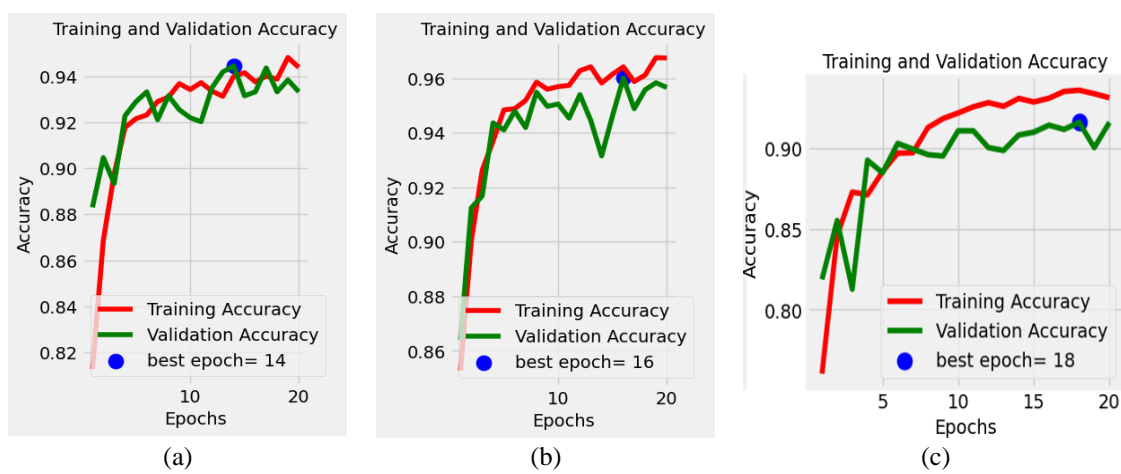


Figure 4. Chart visualizing: (a) InceptionV3, (b) ResNet-50, and (c) MobileNetV3 performances for training and validation accuracies on 3 Subclass

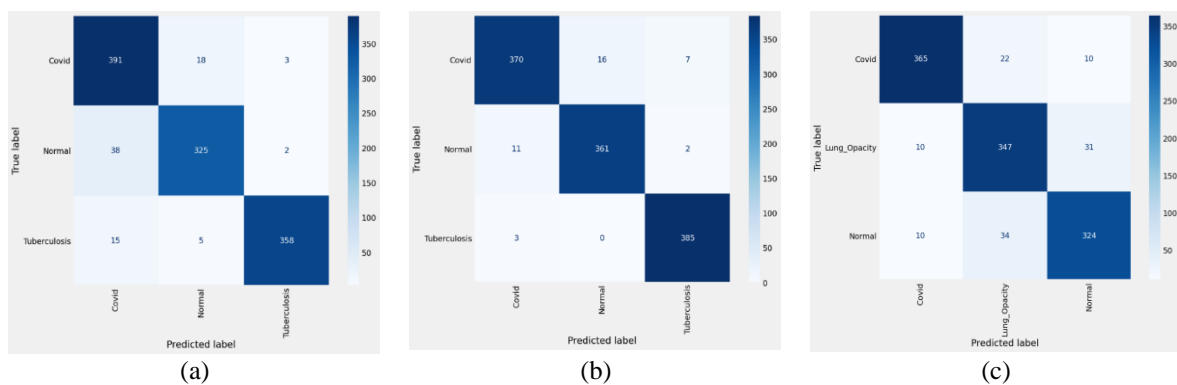


Figure 5. Confusion matrix visualizing: (a) MobileNetV3, (b) ResNet-50 and (c) InceptionV3 performances on Classifying 3 Subclasses

3.1.2. 4-Subclass classification models

This section explores the InceptionV3, ResNet-50 and MobileNetV3 performances for training and validation of losses, accuracies and as well as confusion matrix visualizing on 4 Subclass effectiveness in classifying pulmonary diseases from X-rays in a 4-subclass scenario (COVID-19, lung opacity, normal and tuberculosis) as depicted Figures 6-8. As shown in Figures 6(a), 7(a), and 8(a), the evaluation results reveal

promising performance from the InceptionV3 model on 4-subclass classification. The overall accuracy of 0.89 indicates that the model correctly classified 89% of the samples. Both macro and weighted averages for precision, recall, and F1-score are all 0.89, which suggests that the model performs well on average across all classes. Firstly, the COVID class has the lowest score (89% precision, 83% recall, and 86% F1-score); indicating that the model may have some difficulty in accurately classifying Covid cases compared to the other classes. Secondly, the lung opacity class had the following scores: 89% precision, 83% recall and 86% F1-score. Then, the normal class achieved moderately high scores (93% precision, 89% recall, and 91% F1 score), indicating that the model can reasonably identify normal cases. Finally, the Tuberculosis class has the highest (97% precision, 96% recall, and 96% f1-score), suggesting that the model may have some challenges accurately classifying normal cases due to subtle variations within this category.

Figures 6(b), 7(b), and 8(b) show the 4-subclass classification ResNet-50 task, with an overall accuracy of 91%, which indicates that the model correctly classified a significant portion of the samples in the dataset. Both macro and weighted averages for precision, recall and F1-score reach 0.93, suggesting good average performance across all classes. The weighted average additionally confirms this with potential class imbalances considered. Firstly, the COVID-19 classification scores were 98% precision, 92% recall, and 95% F1-score. This suggests a good ability to identify COVID-19 cases. Thirdly, the lung opacity class achieved moderately high scores (92% precision, 90% recall, and 91% F1-score), demonstrating the model's capability to identify lung opacity cases with reasonable accuracy. Fourthly, the normal class was the second lowest (88% precision, 92% recall, and 90% F1-score). This indicates some challenges in accurately classifying normal cases, potentially due to subtle variations within this category. Finally, the tuberculosis class achieved the highest scores (97% precision, 100% recall, and 98% F1-score), displaying the model's effectiveness in identifying tuberculosis cases. The evaluation results demonstrate promising performance from the proposed model. The overall accuracy of 92% indicates that the model correctly classified a significant portion of the samples in the dataset. Both macro and weighted averages for precision, recall and F1-score reach 0.92, suggesting good average performance across all classes. The weighted average additionally confirms this with potential class imbalances considered.

MobileNetV3 results for 4-subclass classification are shown in Figures 6(c), 7(c), and 8(c). The overall accuracy of 91% indicates that the model correctly classified a significant portion of the samples in the dataset. Both macro and weighted averages for precision, recall and F1-score reach 0.93, suggesting good average performance across all classes. The weighted average additionally confirms this with potential class imbalances considered. The COVID-19 classification scores were 98% precision, 92% recall, and 95% F1-score. This suggests a good ability to identify COVID-19 cases. Thirdly, the lung opacity class achieved moderately high scores (92% precision, 90% recall, and 91% F1-score), demonstrating the model's capability to identify lung opacity cases with reasonable accuracy. Fourthly, the normal class was the second lowest (88% precision, 92% recall, and 90% F1-score). This indicates some challenges in accurately classifying normal cases, potentially due to subtle variations within this category. Finally, the tuberculosis class achieved the highest scores (97% precision, 100% recall, and 98% F1 score), showcasing the model's effectiveness in identifying Tuberculosis cases.

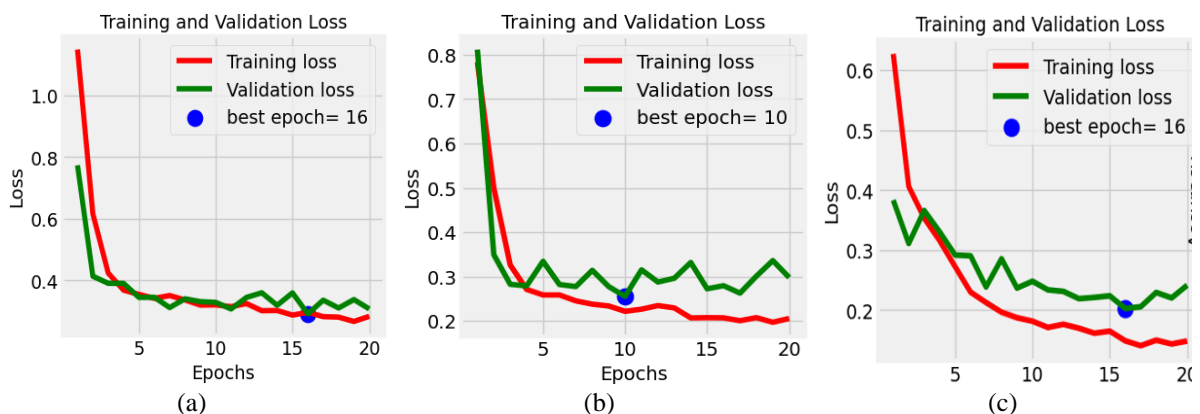


Figure 6. Chart visualizing: (a) InceptionV3, (b) ResNet-50, and (c) MobileNetV3 performances for training and validation losses on 4-Subclass

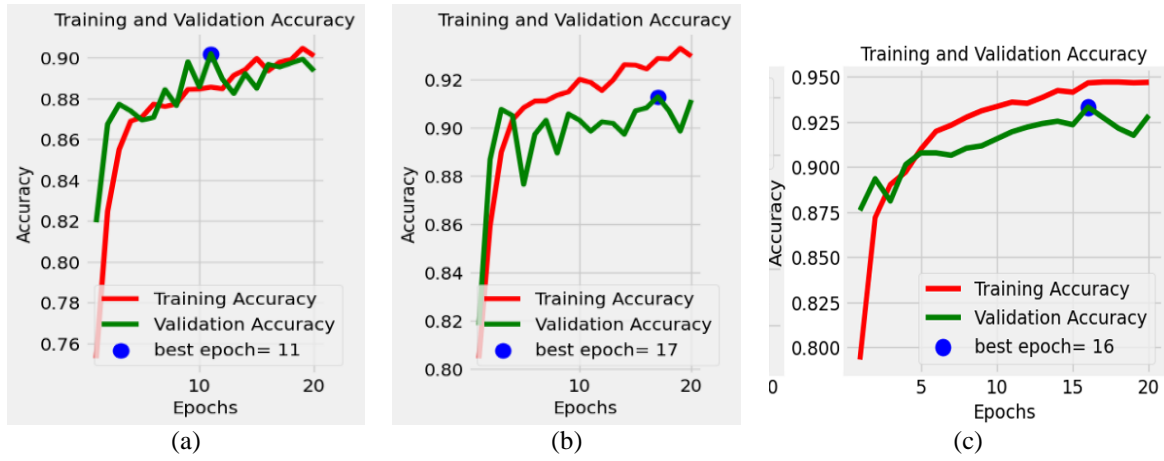


Figure 7. Chart Visualizing: (a) InceptionV3, (b) ResNet-50 and (c) MobileNetV3 performances for training and validation accuracies on 4-Subclass

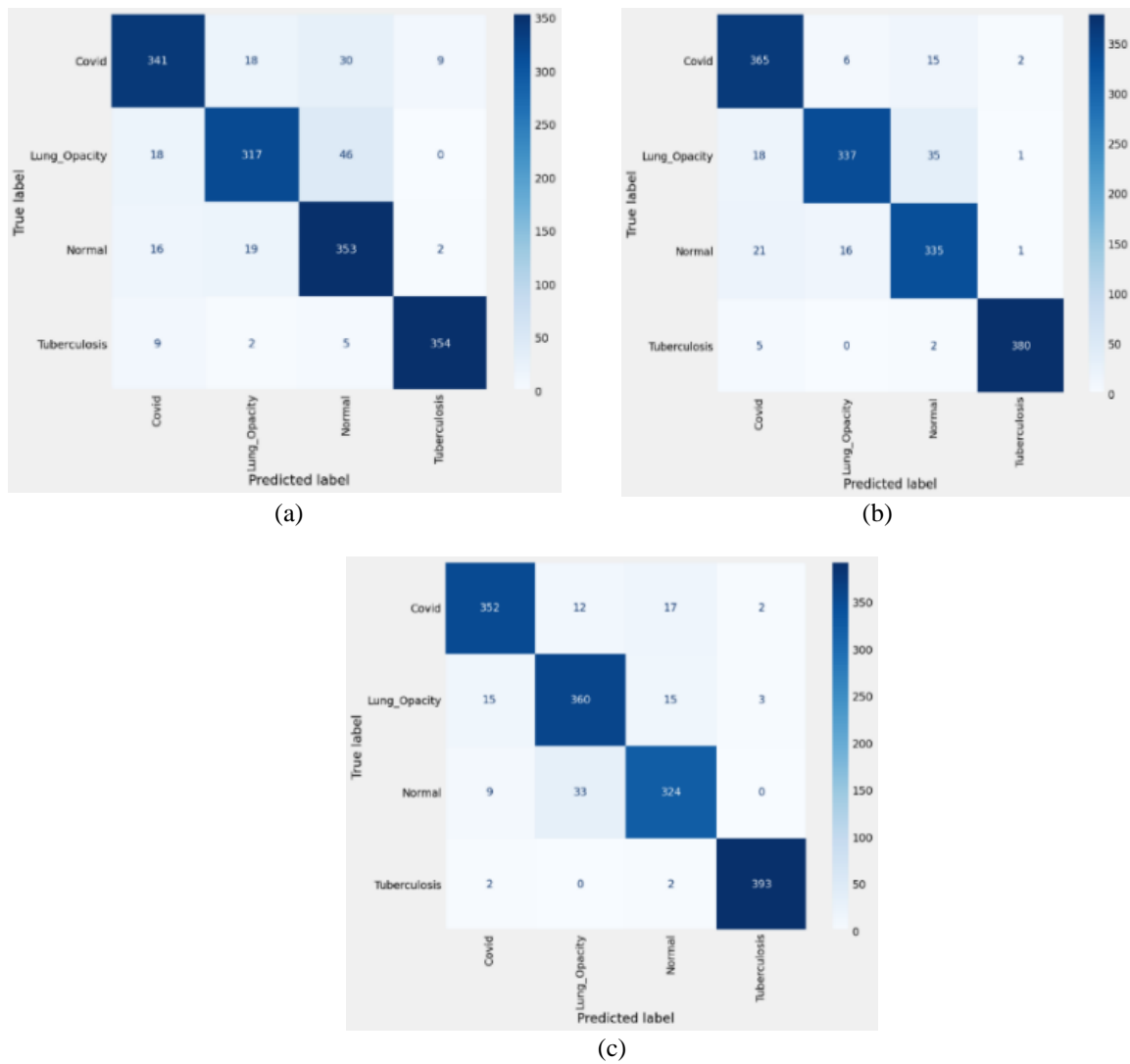


Figure 8. Confusion matrix visualizing: (a) MobileNetV3, (b) ResNet-50, and (c) InceptionV3 performances on classifying 4 subclasses

3.1.3. 5-Subclass classification models

This section explores the InceptionV3, ResNet-50 and MobileNetV3 performances for training and validation of losses, accuracies as well as confusion matrix visualizing on 5-Subclass effectiveness in classifying pulmonary diseases from X-rays in a 5-subclass scenario (bacterial pneumonia, COVID-19, lung opacity, normal and tuberculosis) as depicted Figures 9-11. As shown in Figures 9(a), 10(a), and 11(a), the evaluation results reveal promising performance from the InceptionV3 model on 5-subclass classification. The evaluation's findings show that the InceptionV3 model performs admirably. The model properly identified the samples with an overall accuracy of 90%. The model performs well across all classes, with the weighted average considering class imbalances. The macro and weighted average precision, recall, and F1-score are all 0.90. Firstly, the Pneumonia class achieved the highest scores (98% precision, 98% recall and 98% F1-score), indicating that the model can accurately identify Pneumonia cases. Secondly, the COVID class has a slightly lower score (91% precision, 84% recall and 88% F1-score), indicating that the model may have difficulty accurately classifying COVID cases compared to the other classes. Thirdly, the lung opacity class achieved moderately high scores (84% precision, 83% recall and 83% F1-score), indicating that the model can reasonably identify lung opacity cases. Fourthly, the normal class has the second lowest (82% precision, 86% recall and 84% f1-score), suggesting that the model may have some challenges accurately classifying normal cases due to subtle variations within this category. Finally, the Tuberculosis class has the second highest scores (95% Precision, 98% recall, and 97% f1-score), indicating that the model can effectively identify Tuberculosis cases.

Figures 9(b), 10(b), and 11(b) show the 5-subclass classification ResNet-50 task; the evaluation results reveal promising performance from the proposed model. The overall accuracy of 0.93 indicates that the model correctly classified 93% of the samples. Both macro and weighted average precision, recall, and F1-score are all 0.93, and this suggests that the model performs well on average across all classes, with the weighted average additionally accounting for potential class imbalances. Firstly, the Pneumonia class achieved the highest scores (99% precision, 98% recall and 98% F1-score), indicating that the model can accurately identify Pneumonia cases. Secondly, the COVID class has a slightly lower score (89% precision, 93% recall and 91% F1-score), indicating that the model may have difficulty accurately classifying COVID cases compared to the other classes. Thirdly, the lung opacity class achieved moderately high scores (86% precision, 89% recall and 88% F1-score); indicating that the model can reasonably identify lung opacity cases. Fourthly, the normal class has the second lowest (89% precision, 84% recall and 86% f1-score), suggesting that the model may have some challenges accurately classifying normal cases due to subtle variations within this category. Finally, the Tuberculosis class has the second highest scores (99% Precision, 100% recall, and 99% f1-score), indicating that the model can effectively identify Tuberculosis cases.

MobileNetV3 results for 5-subclass Classification are as shown in Figures 9(c), 10(c), and 11(c). The overall accuracy of 0.94 indicates that the model correctly classified 94% of the samples. Both macro and weighted average precision, recall, and F1-score are all 0.94, and this suggests that the model performs very well on average across all classes, with the weighted average additionally accounting for potential class imbalances.

Firstly, the Pneumonia class achieved the highest scores (98% precision, 99% recall, and 99% F1-score), indicating that the model can accurately identify Pneumonia cases. Secondly, the COVID class has the second-highest scores (94% precision, 96% recall, and 95% F1-score), indicating that the model can effectively classify COVID cases. The lung opacity class achieved moderately high scores (91% precision, 90% recall, and 90% F1-score), indicating that the model can reasonably identify lung opacity cases. The normal class has the fourth-highest scores (90% precision, 88% recall, and 89% F1-score), suggesting that the model can also accurately classify normal cases. The Tuberculosis class has the highest scores (99% precision, 99% recall, and 99% F1-score), along with the Pneumonia class, indicating that the model can exceptionally identify Tuberculosis cases. The model demonstrates excellent overall performance, with Pneumonia and Tuberculosis classifications being the most successful. The model can also effectively classify COVID, lung opacity, and normal cases, with only minor room for improvement. Further investigation might be beneficial to enhance the model's ability to handle the more challenging classes, such as normal, although its performance in this class is still very high.

Figure 11(a) depicts the confusion matrix for the MobileNetV3 model's five-subclass categorization of lung illnesses. Similarly, Figure 11(b) depicts the confusion matrix for the ResNet50 model's five-subclass categorization of lung illnesses. Finally, Figure 11(c) shows the confusion matrix for the InceptionV3 model's five-subclass categorizations of lung illnesses. These confusion matrices thoroughly summarise the classification performance for each lung-related illness subtype across all three model architectures.

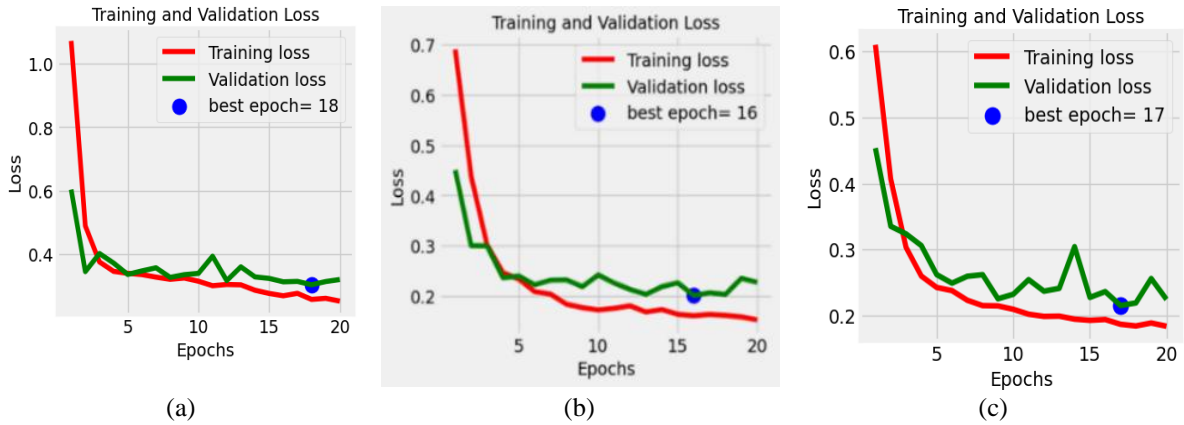


Figure 9. Chart Visualizing: (a) InceptionV3, (b) ResNet-50 and (c) MobileNetV3 performances for training and validation losses on 5-Subclass

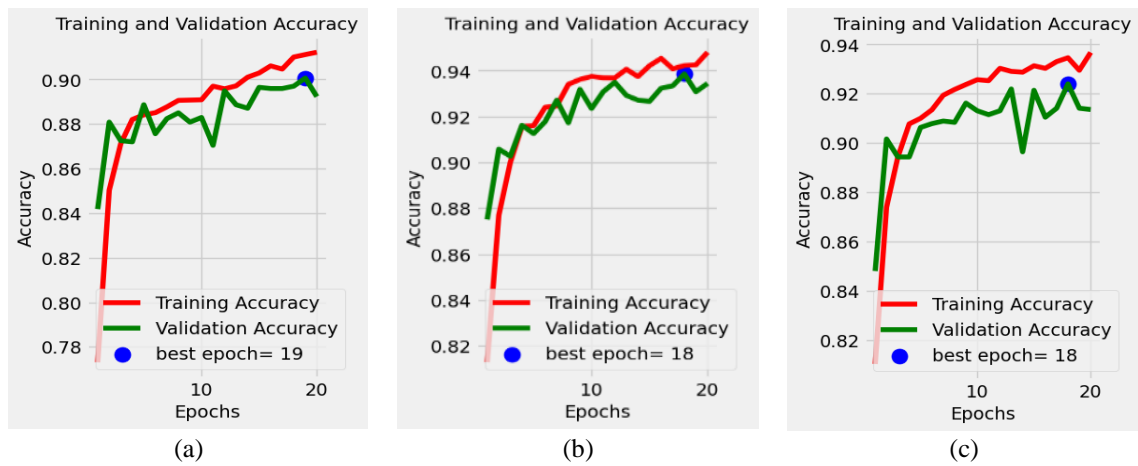


Figure 10. Chart Visualizing: (a) InceptionV3, (b) ResNet-50 and (c) MobileNetV3 performances for training and validation accuracies on 5 Subclass

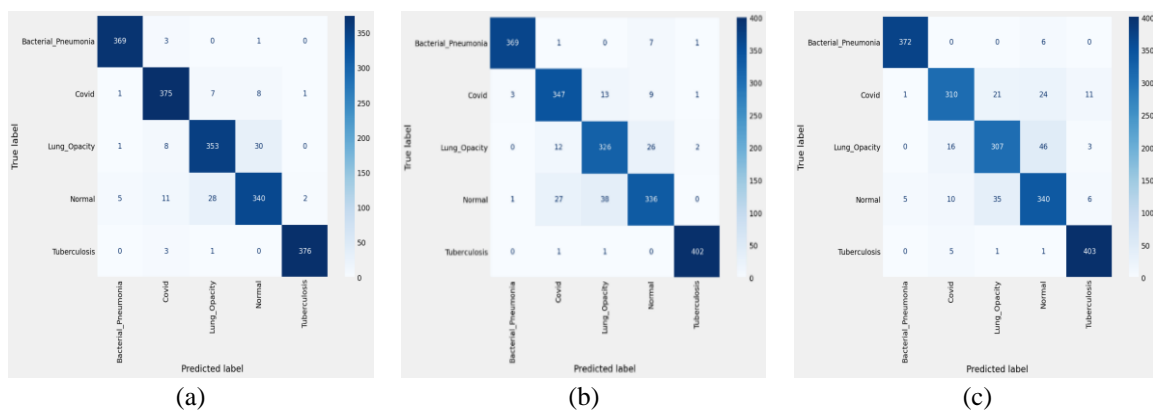


Figure 11. Confusion matrix visualizing: (a) MobileNetV3, (b) ResNet-50, and (c) InceptionV3 performances on classifying 5 subclasses

3.2 Discussion

In the 3-subclass scenario, ResNet-50 achieved the highest precision, recall, F1-score, and accuracy at 96%, 96%, and 96%, respectively. MobileNetV3 and InceptionV3 also performed well, with 90% and 93% across the various metrics. In the 4-subclass scenario, MobileNetV3 outperformed the other models,

achieving 93.75% precision, 93.5% recall, 93.5% F1-score, and 94% accuracy. ResNet-50 and InceptionV3 also demonstrated strong performance, with 92% and 89% accuracy, respectively. For the 5-subclass scenario, MobileNetV3 again showed the best overall performance, with a precision of 94.4%, recall of 94.4%, F1-score of 94.4%, and accuracy of 94.4%. ResNet-50 and InceptionV3 had slightly lower, but still impressive, accuracies of 92.4% and 90%, respectively. These results highlight the potential of these deep learning models, particularly MobileNetV3, in accurately classifying COVID-19, pneumonia, and healthy cases from chest X-ray images, which can be valuable for healthcare professionals in diagnosing and monitoring patients. Table 2 depicts the comparative analysis of various models

Table 2. Comparative analysis of various models

	Metrics	Models		
		MobilNetV3	ResNet50	InceptionV3
3-subClass	Accuracy	90%	96.67%	93%
	Precision	90%	96%	93%
	F1-score	90%	96%	93%
	Recall	90%	96%	93%
4-subclass	Accuracy	94%	92%	89%
	Precision	93.75%	92.2%	89%
	F1-score	93.5%	92.2%	89%
	Recall	93.5%	92%	89%
5-subclass	Accuracy	94.4%	92.4%	90%
	Precision	94.4%	92.4%	90%
	F1-score	94.4%	92.4%	90%
	Recall	94.4%	92.4%	90%

3.3. Model integration into web and mobile applications

The developed deep learning model can be used for practical purposes after a successful model evaluation. Potential integration scenarios include incorporating the model into:

- Software for medical imaging analysis would enable practitioners to use the model's categorization powers in their current procedures.
- Web application: A web application has been developed to offer a user-friendly platform for lung disease classification activities.

3.3.1. A telegram bot for classifying lung diseases

This section shows how to incorporate a deep learning model for user-friendly lung disease classification into a Telegram bot.

- **Functionality:** The Telegram bot uses the pre-trained deep learning model to categorise photographs that users upload. To enable communication with the Telegram network, the bot uses the Python-based Telegram Bot API module.
- **Implementation:** The construction of the bot entails several crucial steps:
 - a) **Library Setup:** Important libraries are imported, including the Telegram API, libraries for image processing, and TensorFlow for deep learning. Furthermore, a logging module is configured to capture pertinent information while the bot is in operation.
 - b) **Model Loading and Preprocessing:** This step loads the pre-trained deep learning model together with the class labels used in the training phase. The `preprocess_image ()` method is used to preprocess user-provided photos. It resizes the image to the required size of the model and normalises the pixel values.
- **Handler Roles:**
 - a) **Start ():** This function receives the `/start` command and responds with a welcome message to users.
 - b) **Predict_and_reply ():** This essential function uses the deep learning model to produce predictions after preprocessing the user's image. The user is then shown the top five anticipated classes.
 - c) **Handle photos () and handle documents ():** These functions deal with the compressed image format (photos) and the uncompressed image format (documents), respectively. The picture data is downloaded, a PIL image object is created, and it is then fed into the `predict_and_reply ()` function.
 - d) **Handle_media_group ():** This function handles media groups (several images in a single message) as a catch-all handler. It recognises the type of media (document or photo) and calls the relevant handler.
 - e) **Principal Role:** By registering the various handlers and starting the polling loop, the `main ()` function sets up the bot. The bot connects to the Telegram network using an API token.
- **Trying out the Bot:** Users can provide a picture (photo or document) of a lung X-ray to the bot to evaluate its performance. The bot in response returns the top five predicted categories, together with the

appropriate confidence scores. To ensure the bot works as expected, it is tested using several image kinds, such as healthy lungs and lungs with various pathologies.

3.3.2. Web application for classifying lung diseases

With the help of a pre-trained deep learning model, users of this programme can submit chest X-rays and receive diagnoses of lung diseases. It blends two essential components:

- JavaScript frontend: constructed using HTML, CSS, and JavaScript, the front end offers an intuitive user experience. Users can:
 - a) Upload an image using a specific element.
 - b) Press a button to start the classification process.
 - c) Examine the classification outcomes as a table or list.
- In the background, JavaScript takes a picture of the submitted file and compresses it (base64) for faster transmission. Makes use of an AJAX request to provide the data to the backend.
- Flask backend: the backend runs server-side processes and is Flask-powered. It gets the frontend's base64-encoded picture data; It decodes the data back into the original format; the trained deep learning model is loaded. Generates predictions on the image using the model. Prepares a response with the highest projected classes together with confidence ratings. Returns the response in JSON format to the front end.

4. CONCLUSION

In this study, three CNN models (ResNet-50, MobileNetV3Small, and InceptionV3) were utilized to analyze and categorize lung illnesses using chest X-ray images. The model leverages chest X-ray images gathered from the Kaggle data repository as well as data published in journals for lung disease diagnosis and management of the diseases by medical experts. The developed DCNN-based multi-classification system for the lung disease diagnosis presented in this study significantly improves chest radiography analysis. The implemented deep-learning approaches revealed the capacity to diagnose various respiratory illnesses from chest X-ray pictures, including pneumonia, TB, and COVID-19. This computer-aided diagnostic tool has the potential to help medical personnel correctly diagnose and manage lung ailments. The first recommendation of this work is that medical professionals and experts must confirm the result from the developed model through their experience. In addition, continuous refinement of the model and adaptation of the model to new sets of data is encouraged through collaborations with relevant stakeholders, regulatory bodies and international organizations in detecting and managing health diseases. In the future, we hope to incorporate multi-modal data such as patient health history into the model to enhance early detection of lung diseases and possible management.

ACKNOWLEDGEMENTS

The authors acknowledge partial assistance from the Covenant University Centre for Research, Innovation, and Discovery (CUCRID), Ota, Ogun State, Nigeria.

FUNDING INFORMATION

No funding involved.

AUTHOR CONTRIBUTIONS STATEMENT

Name of Author	C	M	So	Va	Fo	I	R	D	O	E	Vi	Su	P	Fu
Kennedy Okokpujie	✓	✓	✓	✓	✓	✓	✓	✓	✓	✓	✓	✓	✓	✓
Alvin K. Agamah	✓	✓	✓	✓	✓	✓	✓	✓	✓	✓	✓	✓	✓	✓
Abidemi Orimogunje		✓					✓		✓	✓	✓		✓	✓
Ijeh Princess Adaora		✓					✓		✓	✓	✓		✓	✓
Olusanya Olamide				✓	✓				✓	✓			✓	
Omolara														
Samuel Adebayo					✓		✓			✓			✓	
Daramola														
Morayo Emitha						✓	✓		✓				✓	✓
Awomoyi														

C : C onceptualization	I : I nvestigation	Vi : V isualization
M : M ethodology	R : R esources	Su : S upervision
So : S oftware	D : D ata Curation	P : P roject administration
Va : V alidation	O : O riting - O riginal Draft	Fu : F unding acquisition
Fo : F ormal analysis	E : E riting - R eview & E ditting	

CONFLICT OF INTEREST STATEMENT

No conflict of interest.

INFORMED CONSENT

It is not applicable; secondary datasets were used from the Kaggle repository.

ETHICAL APPROVAL

It is not applicable; secondary datasets were used from the Kaggle repository.

DATA AVAILABILITY

The data supporting this study's findings are openly available in the Kaggle repository at:

- <https://www.kaggle.com/datasets/tawsifurrahman/tuberculosis-tb-chest-xray-dataset> [22].
- <https://www.kaggle.com/datasets/tawsifurrahman/covid19-radiography-database> [23].

REFERENCES

- [1] S. B. Shuvo, S. N. Ali, S. I. Swapnil, T. Hasan, and M. I. H. Bhuiyan, "A lightweight CNN model for detecting respiratory diseases from lung auscultation sounds using EMD-CWT-based hybrid scalogram," *IEEE Journal of Biomedical and Health Informatics*, vol. 25, no. 7, pp. 2595–2603, Jul. 2021, doi: 10.1109/JBHI.2020.3048006.
- [2] R. Bassiouny, A. Mohamed, K. Umopathy, and N. Khan, "An interpretable neonatal lung ultrasound feature extraction and lung sliding detection system using object detectors," *IEEE Journal of Translational Engineering in Health and Medicine*, vol. 12, pp. 119–128, 2024, doi: 10.1109/JTEHM.2023.3327424.
- [3] J. R. Catterall, "Lung infections bullet 5: streptococcus pneumoniae," *Thorax*, vol. 54, no. 10, pp. 929–937, Oct. 1999, doi: 10.1136/thx.54.10.929.
- [4] V. A. Binson, M. Subramoniam, Y. Sunny, and L. Mathew, "Prediction of pulmonary diseases with electronic nose using SVM and XGBoost," *IEEE Sensors Journal*, vol. 21, no. 18, pp. 20886–20895, Sep. 2021, doi: 10.1109/JSEN.2021.3100390.
- [5] I. H. Sarker, "Machine learning: algorithms, real-world applications and research directions," *SN Computer Science*, vol. 2, no. 3, p. 160, May 2021, doi: 10.1007/s42979-021-00592-x.
- [6] M. E. Awomoyi, S. Joshua, K. Okokpujie, A. O. M. Adeoye, A. V. Akingunsoye, and I. P. Okokpujie, "Development of an artificial intelligent health chatbot for improved telemedicine," *Smart Innovation, Systems and Technologies*, vol. 379, pp. 585–600, 2024, doi: 10.1007/978-981-99-8612-5_48.
- [7] B. Abraham and M. S. Nair, "Computer-aided detection of COVID-19 from X-ray images using multi-CNN and Bayesnet classifier," *Biocybernetics and Biomedical Engineering*, vol. 40, no. 4, pp. 1436–1445, Oct. 2020, doi: 10.1016/j.bbe.2020.08.005.
- [8] L. Visuña, D. Yang, J. Garcia-Blas, and J. Carretero, "Computer-aided diagnostic for classifying chest X-ray images using deep ensemble learning," *BMC Medical Imaging*, vol. 22, no. 1, p. 178, Oct. 2022, doi: 10.1186/s12880-022-00904-4.
- [9] C. C. Peng and J. W. Wu, "Deep learning-assisted lung cancer diagnosis from histopathology images," in *2023 IEEE 5th Eurasia Conference on Biomedical Engineering, Healthcare and Sustainability, ECBIOS 2023*, IEEE, Jun. 2023, pp. 17–20. doi: 10.1109/ECBIOS57802.2023.10218594.
- [10] H. Malik, T. Anees, and Mui-zzud-din, "BDCNet: multi-classification convolutional neural network model for classification of COVID-19, pneumonia, and lung cancer from chest radiographs," *Multimedia Systems*, vol. 28, no. 3, pp. 815–829, Jun. 2022, doi: 10.1007/s00530-021-00878-3.
- [11] S. Tang *et al.*, "EDL-COVID: Ensemble deep learning for COVID-19 case detection from chest x-ray images," *IEEE Transactions on Industrial Informatics*, vol. 17, no. 9, pp. 6539–6549, Sep. 2021, doi: 10.1109/TII.2021.3057683.
- [12] E. Khan, M. Z. U. Rehman, F. Ahmed, F. A. Alfouzan, N. M. Alzahrani, and J. Ahmad, "Chest x-ray classification for the detection of COVID-19 using deep learning techniques," *Sensors*, vol. 22, no. 3, p. 1211, Feb. 2022, doi: 10.3390/s22031211.
- [13] J. O. Olayiwola, J. A. Badejo, K. Okokpujie, and M. E. Awomoyi, "Lung-related diseases classification using deep convolutional neural network," *Mathematical Modelling of Engineering Problems*, vol. 10, no. 4, pp. 1097–1104, 2023, doi: 10.18280/mmep.100401.
- [14] R. Careem, G. Johar, and A. Khatibi, "Deep neural networks optimization for resource-constrained environments: techniques and models," *Indonesian Journal of Electrical Engineering and Computer Science*, vol. 33, no. 3, pp. 1843–1854, Mar. 2024, doi: 10.11591/ijeecs.v33.i3.pp1843-1854.
- [15] M. A. A. Al-qaness *et al.*, "Chest x-ray images for lung disease detection using deep learning techniques: a comprehensive survey," *Archives of Computational Methods in Engineering*, vol. 31, no. 6, pp. 3267–3301, Aug. 2024, doi: 10.1007/s11831-024-10081-y.

- [16] M. Harahap *et al.*, "Skin cancer classification using EfficientNet architecture," *Bulletin of Electrical Engineering and Informatics*, vol. 13, no. 4, pp. 2716–2728, Aug. 2024, doi: 10.11591/eei.v13i4.7159.
- [17] J. Oktavian, M. E. Johan, and H. Setiawan, "Integrated map-based system using decision trees and random forests to classify network service issues in telecommunications infrastructure," in *2024 8th International Conference on Information Technology, Information Systems and Electrical Engineering, ICITISEE 2024*, IEEE, Aug. 2024, pp. 93–98. doi: 10.1109/ICITISEE63424.2024.10730407.
- [18] F. M. Al-Matarneh, "Integrating hybrid bald eagle crow search algorithm and deep learning for enhanced malicious node detection in secure distributed systems," *Scientific Reports*, vol. 15, no. 1, p. 12647, Apr. 2025, doi: 10.1038/s41598-025-93549-6.
- [19] M. Loey, F. Smarandache, and N. E. M. Khalifa, "Within the lack of chest COVID-19 X-ray dataset: A novel detection model based on GAN and deep transfer learning," *Symmetry*, vol. 12, no. 4, p. 651, Apr. 2020, doi: 10.3390/SYM12040651.
- [20] H. Malik, T. Anees, M. Din, and A. Naeem, "CDC_Net: multi-classification convolutional neural network model for detection of COVID-19, pneumothorax, pneumonia, lung Cancer, and tuberculosis using chest X-rays," *Multimedia Tools and Applications*, vol. 82, no. 9, pp. 13855–13880, Apr. 2023, doi: 10.1007/s11042-022-13843-7.
- [21] K. H. Shibly, S. K. Dey, M. T. U. Islam, and M. M. Rahman, "COVID faster R-CNN: A novel framework to diagnose novel coronavirus disease (COVID-19) in x-ray images," *Informatics in Medicine Unlocked*, vol. 20, p. 100405, 2020, doi: 10.1016/j.imu.2020.100405.
- [22] "Tuberculosis (TB) chest x-ray database." Accessed: Jul. 19, 2024. [Online]. Available: <https://www.kaggle.com/datasets/tawsifurrahman/tuberculosis-tb-chest-xray-dataset>
- [23] "COVID-19 radiography database." Accessed: Jul. 19, 2024. [Online]. Available: <https://www.kaggle.com/datasets/tawsifurrahman/covid19-radiography-database>
- [24] T. Rahman *et al.*, "Exploring the effect of image enhancement techniques on COVID-19 detection using chest X-ray images," *Computers in Biology and Medicine*, vol. 132, p. 104319, May 2021, doi: 10.1016/j.combiomed.2021.104319.
- [25] T. Rahman *et al.*, "Reliable tuberculosis detection using chest X-ray with deep learning, segmentation and visualization," *IEEE Access*, vol. 8, pp. 191586–191601, 2020, doi: 10.1109/ACCESS.2020.3031384.
- [26] M. E. H. Chowdhury *et al.*, "Can AI help in screening viral and COVID-19 Pneumonia?," *IEEE Access*, vol. 8, pp. 132665–132676, 2020, doi: 10.1109/ACCESS.2020.3010287.

BIOGRAPHIES OF AUTHORS



Dr. Kennedy Okokpujie    holds a bachelor of engineering (B.Eng.) in electrical and electronics engineering, master of science (M.Sc.) in electrical and electronics engineering, master of engineering (M.Eng.) in electronics and telecommunication engineering and master of business administration (MBA), Ph.D. in information and communication engineering, besides several professional certificates and skills. He is currently an associate professor in the department of electrical and information engineering at Covenant University, Ota, Ogun State, Nigeria. He is a member of the Nigeria society of engineers and a senior member of the Institute of Electrical and Electronics Engineers (SMIEEE). His research areas of interest include biometrics, artificial intelligence, and network security and management. He can be contacted at email: kennedy.okokpujie@covenantuniversity.edu.ng, kenjie451@gmail.com.



Alvin K. Agamah    holds a degree in electrical and information engineering from Covenant University, Ota, Nigeria. As a software engineer at Christ Embassy's International School of Ministry and Loveworld Music and Arts Department, he has developed responsive web platforms and dashboards to enhance global outreach. For his undergraduate research, he built a web and mobile application for classifying infectious lung diseases using convolutional neural networks on chest X-ray images. His research interests include software engineering, software testing, and the integration of machine learning into software development, with a focus on healthcare applications using computer vision and AI. Proficient in Python, PHP, JavaScript, TensorFlow, Keras, and Git, Mr. Alvin aims to advance intelligent systems and secure software design to improve digital infrastructure globally. He can be contacted at email: alvin.agamah@stu.cu.edu.ng.



Abidemi Orimogunje    holds a bachelor of science degree in electrical and electronic engineering and a master of science degree in electrical and electronic engineering, both from the University of Ibadan, Nigeria. He is a lecturer and researcher at the department of electrical and electronic engineering, Redeemer's University, Ede, Nigeria. He is a member of the Institute of Electrical & Electronics Engineers (IEEE) and the Nigerian Society of Engineers (NSE). His research areas are signal processing, machine learning, wireless communication, and the internet of things. He can be contacted at email: orimogunje@run.edu.ng.



Ijeh Princess Adaora    is a postgraduate student currently pursuing a master's degree in computer science. She holds a bachelor's degree in computer science from the Federal University of Petroleum Resources, Effurun, Delta State, Nigeria. For her undergraduate research, she developed a web-based electronic management application aimed at improving administrative efficiency. Her current research interests include cybersecurity and artificial intelligence, with a focus on developing smart, data-driven systems. Miss Adaora is dedicated to advancing intelligent technologies through secure and innovative software solutions. She aspires to contribute to cutting-edge research in intelligent systems and secure software design, with the long-term goal of enhancing digital infrastructure in both developing and developed regions. She can be contacted at email: adaora.ijehpgs@stu.cu.edu.ng.



Olusanya Olamide Omolara    holds a bachelor's degree in computer engineering from Ladoke Akintola University of Technology, Ogbomoso, Nigeria, in 2008. Following this, she obtained a master's degree in computer science from the University of Lagos in 2011, and a Ph.D. in computer science in 2017 from Ladoke Akintola University of Technology, Ogbomoso, where she researched the modeling of bank cash deposit transactions using Hierarchical Timed Colored Petri Nets. This research allowed her to explore the intricate dynamics of financial systems and their interactions with technology, equipping her with expertise in system modeling and simulation. Her main interest is in system modeling and simulation and her minor area includes embedded system design and information systems. She is currently lecturing in the department of computer engineering at Bells University of Technology, Ota, Ogun State, Nigeria. She is a member of the Nigeria Society of Engineers and the Institute of Electrical and Electronics Engineers (IEEE). She can be contacted at email: oolusanya@bellsuniversity.edu.ng, olamide4jc@yahoo.com.



Samuel Adebayo Daramola    is a professor of computer engineering. He obtained a Ph.D. from Covenant University in 2008. He obtained a master's degree in engineering (M.Eng.) and bachelor's degree in engineering (B.Eng.) from the University of Port Harcourt in 2002 and Ondo State University in 1997, respectively. He is the former dean of engineering, director of information communication technology (ICT) and head of the computer vision research group at Achievers University Owo. Currently, he is a lecturer at the department of electrical and information engineering (EIE), college of engineering, Covenant University Canaan Land, Ota Nigeria. His research area is computer vision, web-application, Biomedical image processing and software development. He is a member of the Nigeria Society of Engineers (NSE) and the International Association of Engineers (IAENG). He can be contacted at email: samuel.daramola@covenantuniversity.edu.ng.



Morayo Emitha Awomoyi    is a dedicated advocate for social transformation, holding a master's degree in international peace and conflict resolution from American University in Washington, D.C. With a strong academic foundation and a passion for driving meaningful change, Morayo Awomoyi focuses on the intersection of peacebuilding, social justice, and community empowerment. Throughout her career, Morayo Awomoyi has explored innovative approaches to addressing systemic inequalities, fostering inclusive dialogue, and promoting sustainable peace in diverse contexts. She brings a global perspective to local challenges, drawing on both theory and practical engagement in the field of conflict resolution through statistical analyses. Guided by the belief that lasting peace is rooted in equity and social change, Morayo Awomoyi collaborates with communities, organisations, and policy-makers to cultivate environments where justice and human dignity thrive. She can be contacted at email: ma8161b@american.edu.